Journal of Ultrafine Grained and Nanostructured Materials
https://jufgnsm.ut.ac.ir
Vol. 52, No.1, June 2019, pp. 98-109
Print ISSN: 2423-6845 Online ISSN: 2423-6837
DOI: 10.22059/JUFGNSM.2019.01.11

Development and Characterization of Nanocomposite Membranes based on Chitosan, Polystyrene and Montmorillonite for Pervaporation Separation of Phenol and Chlorophenols from Water

Shafagh Mokhtarzadeh*[,1], Farahman Hakimpour*[,1], Samira Agbolaghi[2], Yaghoub Mansourpanah[1],

[1]*Membrane Research Laboratory, Lorestan University, Khorramabad, Iran.*

[2]*Chemical Engineering Department, Faculty of Engineering, Azarbaijan Shahid Madani University, Tabriz, Iran.*

Recieved: 24 December 2018; Accepted: 05 May 2019

** Corresponding author email: shafagh.mo2930@gmail.com*

ABSTRACT

The novel nanocomposite membranes were successfully prepared by the incorporation of different concentrations (5, 10, and 15 wt%) of montmorillonite (MMT) as a nanoadditive into a blend of chitosan/polystyrene (CS/PS) at a ratio of 3:1 on the basis of solution-casting method and they were subsequently used for the separation of phenol, p-chlorophenol, and 2,4-dichlorophenol from water through pervaporation process. The effects of feed composition, the MMT content, and various feed types were investigated on pervaporation performance. All the membranes were water selective and the permeation rate increased with increasing the MMT content. The presence of MMT, increased the hydrophilicity of CS/PS blend polymer matrix, resulting in the formation of a higher flux to water molecules. The best separation performance was achieved for the CS/PSMMT-15 nanocomposite membrane containing a 15 wt % of MMT with 2,4-dichlorophenol in the feed, i.e., the 2,4-dichlorophenol concentration from 0.1 to 0.4 wt %, the flux values from 10.7 to 14.2 g/m^2.h and the separation factor from 1784 to 721. The separation of 2,4-dichlorophenol/water mixture proceeded easier than that of the phenol/water and p-chlorophenol/water mixtures because of the larger molecular size of 2,4-dichlorophenol and the relatively weak coupling

Keywords: *Pervaporation; Phenol and Chlorophenols; Chitosan; Nanocomposite membrane; Montmorillonite.*

1. Introduction

Phenol is used as a general disinfectant for the manufacture of dyes, medical and artificial resins. Phenol, p-chlorophenol and 2,4-dichlorophenol are also applied in the manufacture of textiles, explosives, pharmaceuticals, fertilizers, paints and drugs [1,2]. The chlorinated phenolic compounds are extensively employed in the pesticides industries, thereby water in agriculture fields and effluents generated by such industries gets contaminated with such toxic compounds [3]. Chlorinated phenolic compounds are extremely dangerous than phenol. At low concentrations in water, both p-chlorophenol and 2,4-dichlorophenol are highly toxic [4-5]. Environmental protection agency (EPA) has limited the maximum contamination level of

chlorophenols in water to 0.3 ppm. Therefore, their separation is more essential when they are present in low concentration in water. For removal of these compounds from water, the pervaporation is the best way [6].

The pervaporation (PV) is an excellent membrane technology of liquid mixture separation that is more energy saving, environmentally safe and low operation cost process [7]. The separation mechanism in this technology is based on the difference in sorption and diffusion characteristics of the permeating components [8]. The separation of mixtures by means of pervaporation methods can be classified into three main fields, (i) separation of organic-organic solvent mixtures, (ii) dehydration of aqueous-organic mixtures and (iii) removal of trace volatile organic compounds from aqueous solution [9-10]. According to the solution diffusion model, the permselectivity of a membrane is related to solubility and diffusivity. Therefore, the efficiency of the pervaporation technique depends basically on the inherent properties of the polymers utilized in the fabrication of membrane [11].

The biopolymer-based membranes have unique properties including biocompatibility, biodegradability, good chemical, thermal stability and non-toxicity [12-14]. Recently, the polysaccharides such as chitosan (CS) are getting much attention in different areas. The main source of obtaining chitosan is through the alkaline deacetylation of chitin [15]. This is abundant in nature principally in shells of crustaceans and terrestrial invertebrates. It also used in a wide range of applications such as food, drug, and pharmaceutical fields owing to its extremely high affinity towards water, good film forming properties, non-toxicity, biodegradability, biocompatibility and antibacterial properties [16]. The amino and hydroxyl groups of chitosan can act as electron donors. Because of its high hydrophilicity, chitosan is a good material for preparation of pervaporation membranes [17].

On the other hand, polystyrene (PS) is the most employed aromatic thermoplastic polymer and exhibits many admirable properties such as strong adsorption ability, nontoxicity, biocompatibility, high surface area and chemical inertness. PS membranes demonstrated excellent permeability to the aromatic compounds compared to that of their homologous aliphatic hydrocarbons due to the higher affinity between the two components [18]. To prepare a good membrane for selective removal of water via pervaporation, many methods of membrane modification have been reported subsuming the copolymerization, polymer blending, introduction of bulky pendent groups into the polymer backbone, etc. Blending is an ideal and easy method to produce a membrane with appropriate properties for separation of a mixture [19]. In addition, the combination of nanoscale fillers with polymers may result in advantages such as high resistance, flexibility, appropriate moldability and chemical/thermal stability [20]. Some of these fillers are TiO_2, zeolite, carbon molecular sieve, carbon nanotube (CNT) and graphite [21]. Among different fillers, the montmorillonite (MMT) is a kind of mineral clay and belongs to the general family of 2:1 layered silicates made up of two silica tetrahedral sheets merged to an edge-shared octahedral sheet of alumina or magnesia [22]. The MMT demonstrates a large swelling behavior for its expanded surface area, leading to strong interactions between polymer matrix and clay. It shows good adsorbability, cation exchange capacity and drug carrying capability and is environmental friendly [23]. To our best knowledge, there is no report on the the separation of phenol and chlorophenols using CS/PS/MMT nanocomposite membranes. In this study, the CS/PS/MMT nanocomposite membranes with different amounts of montmorillonite (MMT) were prepared by solution-casting method for the selective removal of phenol, p-chlorophenol and 2,4-dichlorophenol from their aqueous solution by pervaporation. The impacts of feed composition, MMT content, and various feed types were investigated on the pervaporation performance. In addition, the physicochemical properties of membranes were studied using tests of mechanical strength and contact angle.

2. Experimental

2.1. Materials

Chitosan (CS) (N-deacetylation degree 92%, $M_w = 3 \times 10^5$ g/mol) and polystyrene (PS, M_w = 260,000 g/mol) were purchased from Sigma-Aldrich (USA) and used as received. N,N-Dimethylformamide (DMF, 99%) and acetic acid were obtained from Fluka (USA). Montmorillonite (MMT) was purchased from Merk (Darmstadt, Germany). Deionized water was used throughout the research work. The specification of the filler is given in Table 1.

2.2. Preparation of CS/PS membrane and CS/PS/MMT nanocomposite membranes

Blend polymer of chitosan (CS) and polystyrene (PS) was prepared by the following steps. (1) Aqueous CS solution (solution A) was prepared by dissolving of 1.8 g CS in 100 mL of a 2 vol% aqueous acetic acid solution and stirring at room temperature for about 24 h. (2) 1.8 g PS was dissolved in 85 mL DMF (solution B) by stirring for 18 h. (3) The two polymeric solutions containing 5wt% CS/PS with 3:1 weight ratio were initially prepared by mixing solution A and solution B, then stirred under 40 °C for 2h. (4) To prepare the CS/PS/MMT nanocomposite membranes, different amounts of montmorillonite (MMT) (5, 10, 15 wt%) were added into CS/PS blend polymer matrix. The mixed solutions were stirred for about 24 h and then they were kept in an ultrasonic bath for 2 h to break the aggregated crystals of MMT and so as to improve the dispersion of MMT in the blend polymer matrix. The solutions were then filtered and left overnight to get a homogeneous solution. The resulting solutions were poured onto a clean glass plates and the thickness of nanocomposite membranes were adjusted by the casting knife, then dried at room temperature within 24 h. The membranes continued to dry in a vacuum oven at 50 °C for 5 days to remove residual solvent. After complete drying, the blend nanocomposite membranes were peeled off from the glass plate. The amount of MMT varied in 5, 10 and 15 mass % and the obtained membranes were designated as CS/PS unfilled membrane, and CS/PS/MMT-5, CS/PS/MMT-10, CS/PS/MMT-15 nanocomposite membranes. The compositions and physical characteristics of membranes are reported in Table 2.

2.3. Membrane characterization

FT-IR spectra were recorded in the range of 500-4000 cm^{-1} using KBr disc method utilizing a Nicolet-749, Perkin-Elmer 287B FTIR spectrophotometer. Thermal stabilities of CS/PS and CS/PS/MMT-15 nanocomposite membranes were examined (Seiko 220TG/DTA analyzer) in the temperature range of 25-600 °C at a heating rate of 10 °C min^{-1} with continuous flushing under nitrogen gas at 250 mL min^{-1}. The scanning electron microscopic (SEM) images of the CS/PS membrane and CS/PS/MMT nanocomposite membrane were obtained under high resolution (Ma: 300X, 6kv) utilizing a JOEL MODEL JSM 840 A, SEM. A siemens D 5000 powder X-ray diffractometer was applied to estimate the solid-state morphology of CS/PS membrane and CS/PS-MMT-15 nanocomposite membrane in powdered form. X-rays of 1.54 Å wavelengths were generated by a Cuk source. The measurement of the membrane contact angle was carried out on olymus optical microscope camera (B X51, japan) and the angle of the tangent to the droplets relative to the horizon was determined at ambient temperature and repeated for each sample at 3 points of the membrane surface. Tensile strength of membranes was measured using Houndfield H10KS Universal Testing Machine (UTM). According to ASTM specifications, rectangular strips of 6 mm width were cut out from the polymer membrane. The strips were well gripped using thick paper during

Table 1- Specification of the nano-clay

Filler	Montmorillonite
Filler concentration	120 meq/100 g clay
Particle size of clay	91-96 nm
Density	1.68 g/cm^3
Basal spacing	d_{00} is 2.19 nm

Table 2- Compositions and physical characteristics of CS/PS/MMT nanocomposite membranes

Membrane designation	MMT (Wt%)	Contacts angle (degree)	Thickness (μm)	Tensile strength (MPa)
CS/PS	0	74	30	8.97
CS/PS/MMT-5	5	70	30	12.85
CS/PS/MMT-10	10	65	30	19.67
CS/PS/MMT-15	15	61	30	25.08

the measurement of tensile strength.

2.4. Pervaporation measurement

Pervaporation of phenol/water, p-chlorophenol/water and 2,4-dichlorophenol/water mixtures was performed utilizing the standard rig configuration as shown in Fig. 1 [24]. The PV cell was assembled from two cylindrical half cells made of stainless steel. The membranes were supported on a perforated stainless steel plate placed at the junction of two cells. In pervaporation, the feed solution is in direct contact with the membrane. The effective membrane area for PV was 12.6 cm^2. The system was operated at 30 °C and at 6 mm.Hg pressure by using a vacuum pump. The permeate vapor was condensed in a glass condenser suspended inside a cryogenic trap kept at -40° C. Pervaporation separation was carried out at varying feed composition of 0.1 to 0.4 % phenol, p-chlorophenol, and 2,4-dichlorophenol in water. The permeation rate was characterized by measuring the weight of the permeate. The compositions of the feed solution and the permeate were measured by gas chromatography (Varian 3300 gas chromatograph). The permeation flux was measured as follow:

$$P=W/A.t \quad \text{(eq. 1)}$$

where, P, W, A and t indicate the permeation flux (kg/m^2h), weight of permeate (g), effective area based on the outside diameter of the membrane (m^2) and operation time (h), respectively. The permeation flux was determined by dividing the measured weight of the permeate by the sampling time. The separation factor is defined by:

$$\alpha_{A/B} = (Y_A/Y_B)(X_A/X_B) \quad \text{(eq. 2)}$$

where, Y_A and Y_B are the weight fraction of the component in feed and X_A and X_B are the weight fraction of those in the permeate (A being the more permeative species), respectively.

3. Results and discussion

3.1. Fourier transform infrared (FT-IR) studies

FT-IR spectra of the nano clay powder, neat chitosan, neat PS, CS/PS membrane and CS/PS/MMT-15 nanocomposite membrane are

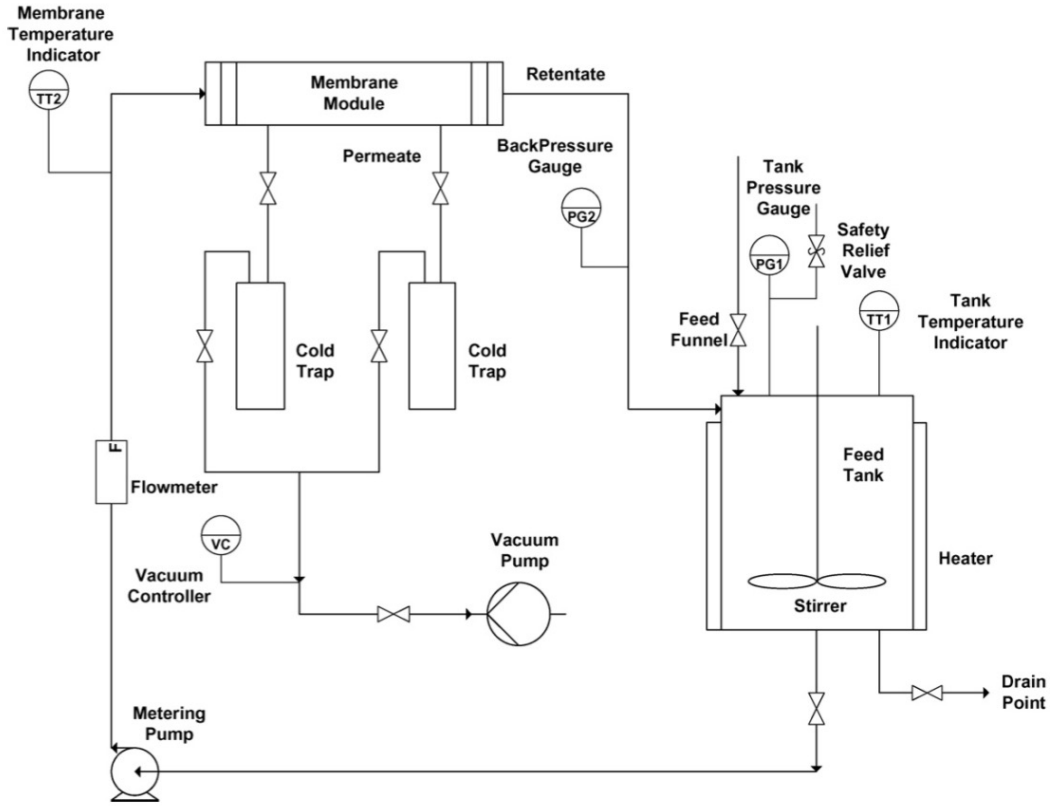

Fig. 1- Schematic representation of pervaporation unit.

represented in Fig. 2. Fig. 2a, displays FT-IR spectra of montmorillonite. The vibration band corresponding to the stretching of hydroxyl groups and cations from the octahedral sheet at 3728 cm^{-1} can be detected. A strong band at 3324 cm^{-1} is a result of the presence of water adsorbed on the clay surface. The absorption peak in the region of 1640 cm^{-1} is assigned to the -OH bending mode of adsorbed water. The characteristic peak at 1115 cm^{-1} is due to the Si-O-Si stretching and the band at 522 cm^{-1} refers to deformation vibrations of Si-O-Al. In the spectrum of chitosan (Fig. 2b), the bands at 3425 cm^{-1} (O-H and N-H stretching vibrations), 1637 cm^{-1} (C=O stretching in amide group), 1547 cm^{-1} (N-H bending in amide group), 1152 cm^{-1} (anti symmetric stretching of the C-O-C bridge), 1060 cm^{-1} and 1024 cm^{-1} (skeletal vibrations involving the C-O stretching) were reported as characteristic bands in the chitosan structure. For the neat PS (Fig. 2c), the spectrum displays the typical characteristic bands for PS at 3020, 2900, 1750 to 2000 and 1610 cm^{-1}, which related to the aliphatic C-H and -CH_2, and the aromatic C=C stretching, respectively. Moreover, a broad peak at 3100-3500 cm^{-1} could be correlated with the aromatic C-H and C=C-H stretching. FT-IR spectrum of the CS/PS membrane (Fig. 2d) is the combination of characteristic bands of spectra of both components. In this spectrum, some characteristic peaks in the PS and CS regions are shifted to higher wavenumbers compared with the neat polymers, an absorption peak at 3084 cm^{-1} corresponding to the C-H stretching vibration on the substituted benzene ring of the styrene moiety of the blend polymer. Likewise, the C=C stretching vibration of the benzene ring is observed at 1455, 1495 and 1602 cm^{-1} and the absorption bands at 699 and 763 cm^{-1} are due to the single substituted benzene ring. At chitosan moiety of the blend polymer, the peak of N-H groups at 3500 cm^{-1} was shifted to 3423 cm^{-1}. Stretching vibration of C-H was also shifted from 2937 to 2820 cm^{-1}.

As could be observed in Fig. 2e, an alteration

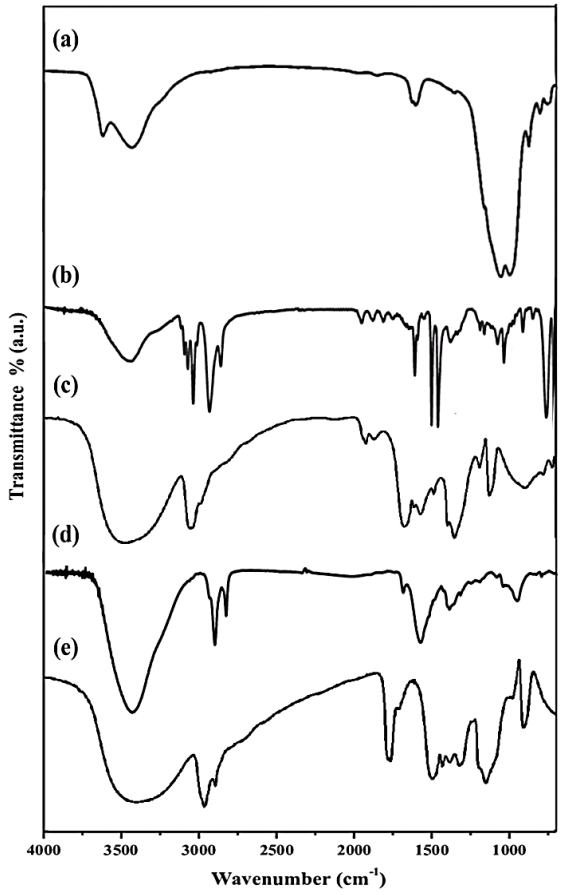

Fig. 2- FT-IR Spectra of (a) MMT, (b) CS, (c) PS, (d) CS/PS unfilled membrane and (e) CS/PS/MMT-15 nanocomposite membrane.

in the spectra of CS/PS-MMT-15 nanocomposite membrane after addition of MMT has been emerged. It also demonstrates an absorption band at 1030 cm^{-1} related to Si-O stretching of the MMT, which was observed at 1324 cm^{-1} in the nanocomposite. Similarly, 523 cm^{-1} band attributed to the stretching of Al-O band of MMT is detected at 900 cm^{-1} in the CS/PS/MMT-15 nanocomposite membrane. Moreover, differences in the position and intensity of bands ranged in 900-1750 cm^{-1} wavenumbers. All these results indicated the presence of chitosan, polystyrene and the MMT in the nanocomposite membrane [25].

3.2. Thermal gravimetric analysis (TGA)

The thermal stabilities of CS/PS unfilled membrane and CS/PS/MMT-15 nanocomposite membrane were analyzed utilizing the thermo gravimetric analysis under the nitrogen atmosphere. The resulting curves are illustrated in Fig. 3. The TGA curve of CS/PS unfilled membrane (see Fig. 3a) represents the weight loss onset at 289 °C followed by a final decomposition at 320 °C. Fig. 3b shows that the CS/PS/MMT-15 nanocomposite membrane undergoes a weight loss starting at 250 °C followed by the final decomposition at 410 °C, which includes the thermal decomposition of CS/PS blend polymer and MMT. The thermal stability of CS/PS/MMT-15 nanocomposite membrane was enhanced compared to CS/PS unfilled membrane. The thermal stability increase of the nanocomposite membrane can be explained by the introduction of montmorillonite into the CS/PS blend polymer matrix and formation of parallel monolayer of MMT, in which the CS/PS blend polymer chains penetrated into the galleries of the clay. The dispersion of CS/PS blend polymer in the silicate layers not only effectively inhibited the permeation of oxygen, but also restricted their thermal motion. This TGA study reveals that the synthesized membranes have satisfactory thermal stability and the membranes can be effectively used in pervaporation experiments, even at high operating temperatures [26].

3.3. Scanning electron microscopy (SEM)

SEM images of CS/PS unfilled membrane and CS/PS/MMT nanocomposite membrane containing 5, 10 and 15 wt% MMT are exhibited in Fig. 4. As shown in Fig. 4a, SEM image of CS/PS unfilled membrane represents smooth and homogeneous morphology and no bulky agglomeration is observed, which demonstrates proper interaction between the two different materials, on the other word this membrane is dense. Figs. 4b to d show the surface membranes prepared by using different amount of montmorillonite as given in Table 2. In CS/PS/MMT-5 nanocomposite membrane (Fig. 4b), where 5% MMT was used, the bright spots on the membrane surface increased by elevating the MMT concentration which illustrates the MMT particles on the top surface of the nanocomposite membrane. Clearly, the MMT content on the membrane surface increased by enhancement

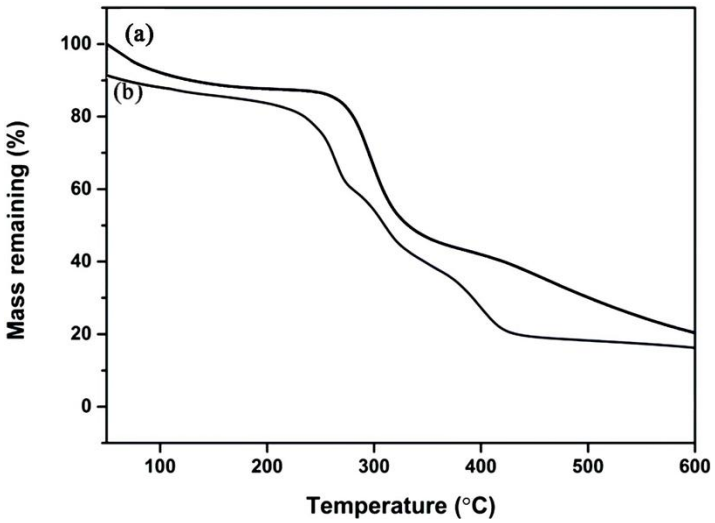

Fig. 3- TGA thermogram of (a) CS/PS unfilled membrane and (b) CS/PS/MMT-15 nanocomposite membrane.

of incorporated MMT into the membranes. The MMT particles were aggregated in CS/PS/MMT-10 nanocomposite membrane (Fig. 4c), where 10% MMT was given. In CS/PS/MMT-15 (Fig. 4d), when the maximum amount of MMT (15%) was used, the agglomeration of MMT particles on the membrane surface was higher than that of the CS/PS/MMT-10. This can be explained with bigger crystal formation from more number of MMT molecules during membrane solidification by solvent evaporation CS/PS/MMT-15 nanocomposite membrane [27].

3.4. XRD analysis

In order to get an idea of the morphological state of the synthesized membranes, X-ray diffraction analysis was carried out. The XRD patterns of CS/PS unfilled membrane, original MMT, and CS/PS-MMT-15 nanocomposite membrane are represented in Fig. 5. As could be observed in Fig. 5a, the broad diffraction peaks of CS/PS unfilled membrane were detected around $2\theta = 5°$, indicating an average intermolecular distance of semicrystalline structure of blend membrane. Fig. 5b shows the XRD pattern of original MMT. The crystalline organoclay filler is observed to show many diffraction peaks. At $2\theta = 7.19°$, there is a strong diffraction peak for MMT. For CS/PS/MMT-15 nanocomposite membrane, the diffraction peak of MMT at $2\theta = 7.19°$ disappeared (Fig. 5c). It suggested that the silicate layers of MMT had entered into the blend polymer matrix. In addition, the other peaks of MMT cannot be detected. The absence of the most of the XRD peaks of clay in the CS/PS/MMT-15 nanocomposite membrane indicates strong electrostatic interaction amongst the functional groups of the nanofiller and the CS/PS blend polymer, which breaks the regular and periodic structure of MMT [28].

3.5. Effect of feed composition on the pervaporation performance

The effect of feed concentration on the permeation flux and separation factor was studied using the CS/PS unfilled membrane and CS/PS/

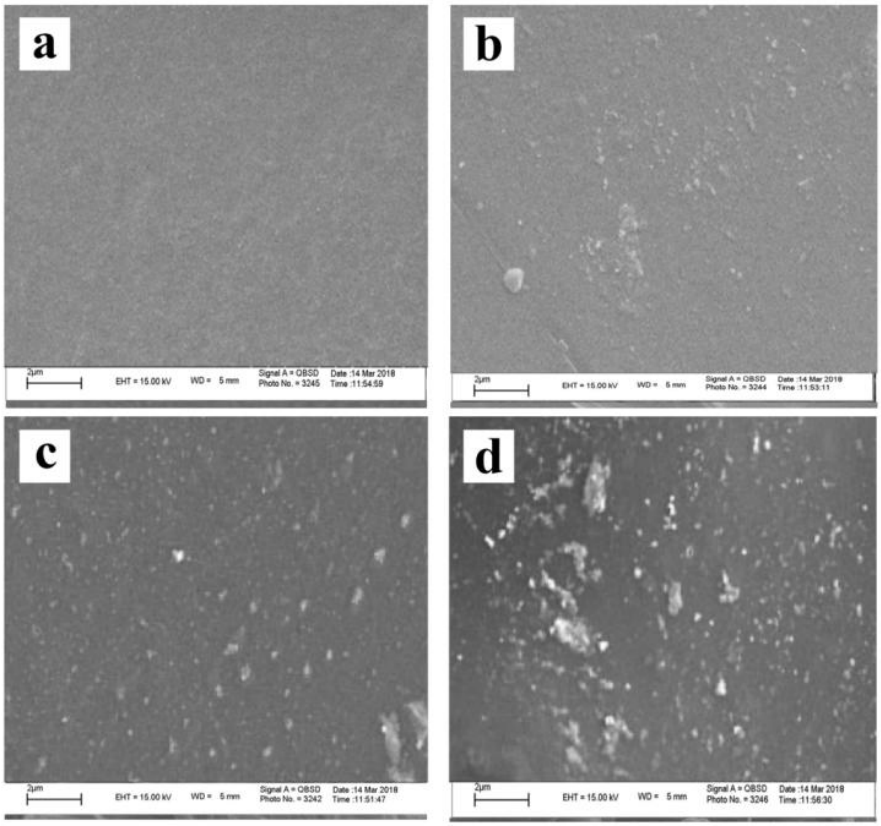

Fig. 4- SEM images of the surface morphologies of (a) CS/PS unfilled membrane; (b) CS/PS/MMT-5 nanocomposite membrane; (c) CS/PS/MMT-10 nanocomposite membrane; (d) CS/PS/MMT-15 nanocomposite membrane.

MMT nanocomposite membrane. Pervaporation experiments were carried out by different feed concentration from 0.1 to 0.4 wt % at 30° C for the separation of phenol, p-chlorophenol and 2,4-dichlorophenol from water and the results are reported in Figs. 6 and 7. In all cases, the flux of phenol and chlorophenols is found to increase with the increase in their concentrations in feed, but separation factor decreased. For example, for CS/PS/MMT-15 nanocomposite membrane with 2,4-dichlorophenol in feed, increase in 2,4-dichlorophenol concentration from 0.1 to 0.4 wt %, increase in the flux value from 10.7 to 14.2 kg/m^2.h, and decrease in separation factor from 1784 to 721 were detected. Likewise, for p-chlorophenol/water mixture, an increase in p-chlorophenol concentration in feed from 0.1 to 0.4 wt %, increase in the flux value from 9.6 to 12.2 kg/m^2.h, and also for phenol/water mixture increase in phenol concentration from 0.1 to 0.4 wt %, increase in the flux values from 8.8 to 11.9 Kg/m^2.h, also decrease in separation factor from 1749 to 701 for p-chlorophenol/water mixture and from 1689 to 692 for phenol/water mixture were observed. It is found that chitosan presence enhanced the hydrophilicity of the prepared nanocomposite membranes because it is hydrophilic. This was also supported from the contact angle measurements. The reason for the improvement in hydrophilicity of the synthesized membrane by adding CS is attributed to hydrophilic functional groups of chitosan, such as hydroxyl and amino groups on the surface of the membranes. As the water concentration in the feed increased the membrane was more swollen. Due to the high hydrophilicity of CS/PS/MMT nanocomposite membranes, the free volume in the polymer increases and the polymer chains become more flexible, thus making the permeant molecules to penetrate through the membrane more easily [29]. Similar results were observed for the CS/PS/MMT-5, CS/PS/MMT-10 and CS/PS/MMT-15 nanocomposite membranes.

3.6. Effect of nanofiller loading on pervaporation performance

With regard to the membrane performance, in the case of CS/PS/MMT nanocomposite membranes, permeability values for phenol, p-chlorophenol

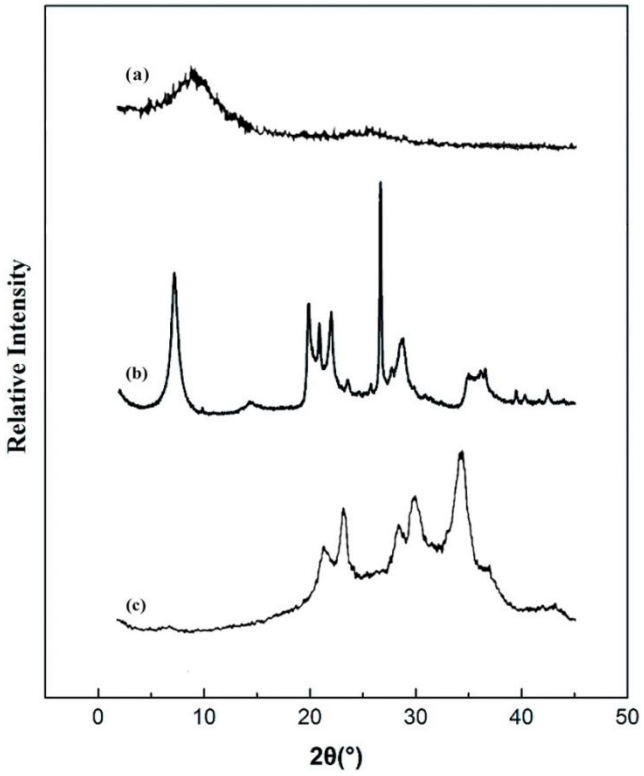

Fig. 5- XRD spectra of (a) CS/PS unfilled membrane, (b) MMT nanofiller, and (c) CS/PS/MMT-15 nanocomposite membrane.

and 2,4-dichlorophenol were higher than the CS/PS unfilled membrane as shown in Figs. 6 and 7. Generally, the permeate fluxes of CS/PS unfilled membranes at 0.4 wt % were 9.4, 10.2, and 10.6 kg/m^2.h for separating phenol, p-chlorophenol and 2,4-dichlorophenol mixtures, at operating conditions, respectively. After incorporation of MMT nanofiller with contents of 5, 10 and 15 wt % for the same feed concentration, the CS/PS/MMT nanocomposite membranes depicted the higher fluxes than those detected for the CS/PS unfilled membranes. The permeate fluxes of CS/PS/MMT nanocomposite membranes at 0.4 wt % for separating the 2,4-dichlorophenol/water mixtures were 11.6, 12.2 and 14.2 kg/m^2.h, as the MMT content were 5, 10 and 15 wt %, respectively. Similar results were observed for separating the phenol/water and p-chlorophenol/water mixtures. The permeate fluxes of CS/PS/MMT nanocomposite membranes at 0.4 wt % for separating phenol/water mixtures were 10.2, 11.2 and 11.9 kg/m^2.h and for p-chlorophenol/water mixtures were 10.8, 11.4 and 12.2 kg/m^2.h, as the MMT content were 5, 10 and 15 wt %, respectively. These results can be explained due to the enhancement of sorption of the membranes toward water molecules. The hydrophilic nanofiller increases the preferential water-membrane interaction. Furthermore, at higher filler loading, the polymer free volume would decrease, leading to enhanced tortuous pathways inside the membranes [30]. Therefore, the CS/PS/MMT nanocomposite membranes are suitable for separation of phenol and chlorophenols from water.

3.7. Effect of different feed types on pervaporation performances of CS/PS/MMT nanocomposite membranes

The separation efficiency of CS/PS/MMT nanocomposite membranes for the separation of

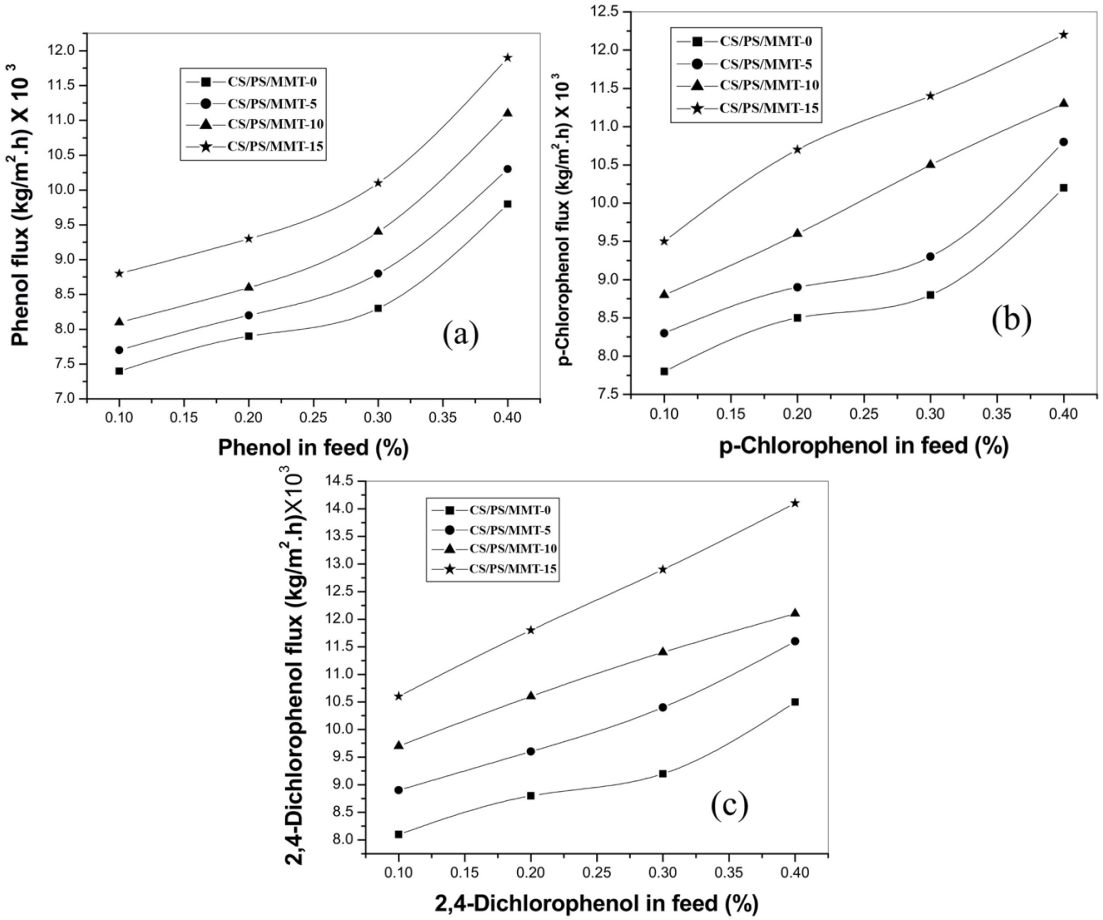

Fig. 6- Variation of phenol flux (a), p-chlorophenol (b), 2,4-dichlorophenol (c), with change in feed concentration for different membranes.

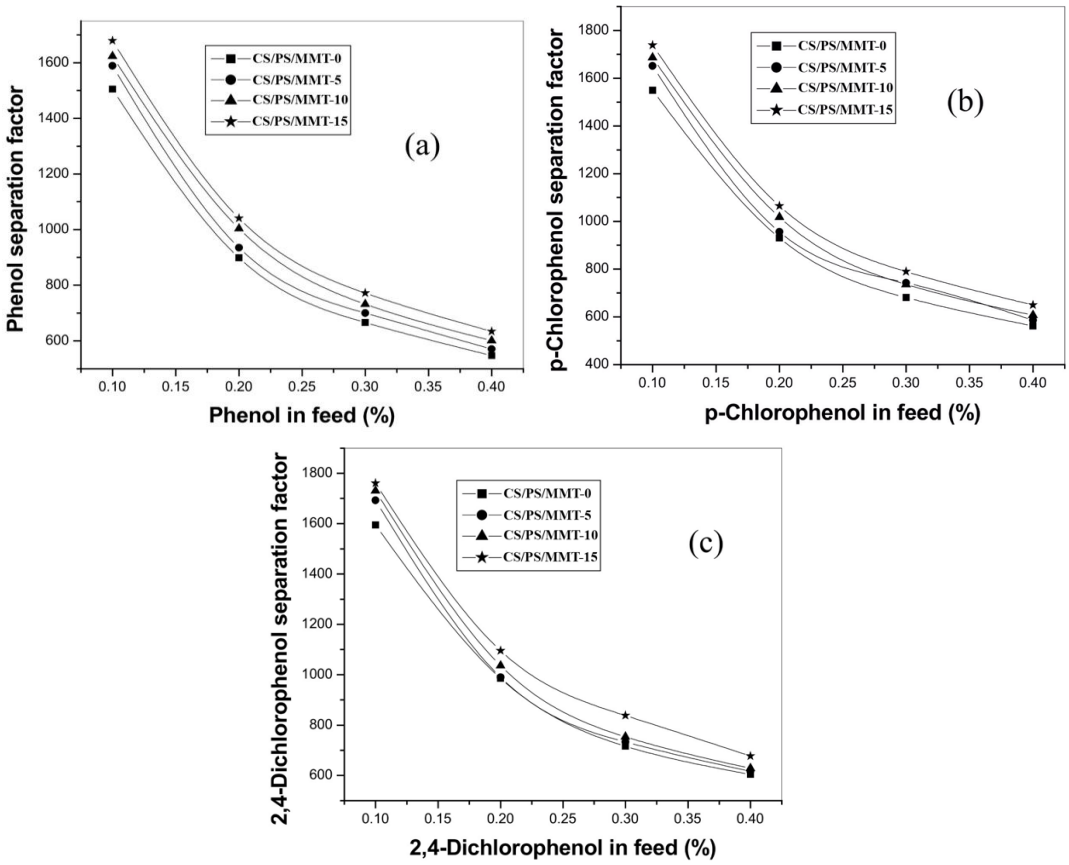

Fig. 7- Variation of separation factor of phenol (a), p-chlorophenol (b), and 2,4-dichlorophenol (c) with alteration in feed concentration for different membranes.

Table 3- Pervaporation fluxes for separation of phenol, p-chlorophenol and 2,4-dichlorophenol from water through CS/PS unfilled membrane, CS/PS/MMT-5, CS/PS/MMT-10 and CS/PS/MMT-15 nanocomposite membranes

Nanocomposite membrane	phenol			p-Chlorophenol			2,4-Dichlorophenol		
	In		Flux	In		Flux	In		Flux
	Feed (%)	Permeate (%)	(Kg/m^2h)	Feed (%)	Permeate (%)	(Kg/m^2h)	Feed (%)	Permeate (%)	(Kg/m^2h)
CS/PS	0.1	62.3	7.5	0.1	63.1	7.9	0.1	63.6	8.2
	0.2	66.5	8.0	0.2	67.4	8.6	0.2	69.5	8.9
	0.3	68.9	8.4	0.3	69.5	8.9	0.3	71.2	9.3
	0.4	70.9	9.4	0.4	72.3	10.2	0.4	73.9	10.6
CS/PS-MMT-5	0.1	63.6	7.8	0.1	64.5	8.4	0.1	65.8	9.0
	0.2	67.4	8.3	0.2	67.9	9.0	0.2	68.3	9.7
	0.3	69.1	8.9	0.3	73.4	9.4	0.3	70.1	10.5
	0.4	71.8	10.4	0.4	74.6	10.9	0.4	74.5	11.7
CS/PS-MMT-10	0.1	64.2	8.2	0.1	64.4	8.9	0.1	65.5	9.8
	0.2	68.5	8.7	0.2	69.3	9.7	0.2	70.2	10.7
	0.3	70.4	9.5	0.3	72.8	10.6	0.3	71.4	11.5
	0.4	72.9	11.5	0.4	73.2	11.4	0.4	73.5	12.2
CS/PS-MMT-15	0.1	64.9	8.8	0.1	65.6	9.6	0.1	65.4	10.7
	0.2	69.8	9.4	0.2	70.2	10.8	0.2	70.7	11.9
	0.3	72.3	10.2	0.3	73.1	11.5	0.3	73.5	12.8
	0.4	74.7	11.9	0.4	75.3	12.2	0.4	75.3	14.2

phenol, p-chlorophenol, and 2,4-dichlorophenol from water at 30 °C are displayed in Figs. 6 and 7. The results demonstrated that for CS/PS/MMT-15 nanocomposite membranes with 0.4 wt % 2,4-dichlorophenol in feed mixture, an increase in the molecular size of phenol and chlorophenols resulted in an increase in the permeation rate from 11.9 kg/m^2.h for phenol to 14.2 kg/m^2.h for 2,4-dichlorophenol. Similar results were acquired for other CS/PS/MMT nanocomposite membranes with 0.4 wt % phenol and chlorophenols in feed mixture. This is also evident from Fig. 7a and Fig. 7b that the highest permeation rate (14.2 kg/m^2.h) was observed for the CS/PS/MMT-15 nanocomposite membrane for separating 2,4-dichlorophenol/water mixtures at 30 °C for 0.4 wt % 2,4-dichlorophenol in the feed. These results indicated that the separation of 2,4-dichlorophenol/water mixture proceeded easier than that of the separation of phenol/water and p-chlorophenol/water mixtures because of the larger molecular size of 2,4-dichlorophenol and relatively weak coupling phenomenon (less polar than phenol and p-chlorophenol) with water molecules and hydrophilic membranes [31]. The higher permeation fluxes for 2,4-dichlorophenol mixtures compared to other two mixtures can be attributed to less polarity and less coupling in the 2,4-dichlorophenol mixtures. Again for the same reasons, the other CS/PS/MMT membranes are more efficient for the separation of phenol and p-chlorophenol from water. The selectivity of CS/PS/MMT nanocomposite membranes towards phenol and chlorophenols followed the order of phenol< p-chlorophenol < 2,4-dichlorophenol.

4. Conclusions

The novel nanocomposite membranes were prepared by incorporating different concentrations (5, 10 and 15 wt%) of MMT as a nanoadditive into a blend of chitosan/polystyrene at ratio of 3:1 (CS/PS) on the basis of solution-casting method. The developed samples were subsequently used for the separation of phenol, p-chlorophenol, and 2,4-dichlorophenol from water through pervaporation process. The prepared nanocomposite membranes were systematically characterized using FT-IR, TGA, SEM, contact angle and mechanical strength. The effects of feed composition, MMT content, and various alcohols on pervaporation performance were investigated. The experimental results revealed that all the membranes were water selective and the permeation rate increased with increasing the MMT content. The presence of MMT increased the hydrophilicity of CS/PS blend, reflecting the formation of a higher flux to water molecules. The best separation performance was achieved for the CS/PSMMT-15 nanocomposite membrane containing 15 wt % MMT with 2,4-dichlorophenol in feed. The separation of 2,4-dichlorophenol/water mixture proceeded easier than that of the phenol/water and p-chlorophenol/water mixtures.

References

1. Roda FAT, Desouky AMAEH, Mona AS. Isolation, biochemical and molecular characterization of 2-chlorophenol-degrading Bacillus isolates. African Journal of Biotechnology. 2007;6(23):2675-81.
2. Bae H. Biodegradation of 4-chlorophenol via a hydroquinone pathway by Arthrobacter ureafaciens CPR706. FEMS Microbiology Letters. 1996;145(1):125-9.
3. Bae HS, Lee JM, Kim YB, Lee S-T. Biodegradation of the mixtures of 4-chlorophenol and phenol by Comamonas testosteroni CPW301. Biodegradation. 1997;7(6):463-9.
4. Becker JG, Stahl DA, Rittmann BE. Reductive dehalogenation and conversion of 2-chlorophenol to 3-chlorobenzoate in a methanogenic sediment community: implications for predicting the environmental fate of chlorinated pollutants. Appl. Environ. Microbiol.. 1999 Nov 1;65(11):5169-72.
5. Bergauer P, Fonteyne P-A, Nolard N, Schinner F, Margesin R. Biodegradation of phenol and phenol-related compounds by psychrophilic and cold-tolerant alpine yeasts. Chemosphere. 2005;59(7):909-18.
6. Cai M, Xun L. Organization and Regulation of Pentachlorophenol-Degrading Genes in Sphingobium chlorophenolicum ATCC 39723. Journal of Bacteriology. 2002;184(17):4672-80.
7. Shao P, Huang RYM. Polymeric membrane pervaporation. Journal of Membrane Science. 2007;287(2):162-79.
8. Smitha B. Separation of organic?organic mixtures by pervaporation?a review*1. Journal of Membrane Science. 2004;241(1):1-21.
9. Chapman PD, Oliveira T, Livingston AG, Li K. Membranes for the dehydration of solvents by pervaporation. Journal of Membrane Science. 2008;318(1-2):5-37.
10. Cao X, Zhang T, Nguyen QT, Zhang Y, Ping Z. A novel hydrophilic polymer-ceramic composite membrane 1. Journal of Membrane Science. 2008;312(1-2):15-22.
11. Qiu W, Kosuri M, Zhou F, Koros WJ. Dehydration of ethanol–water mixtures using asymmetric hollow fiber membranes from commercial polyimides. Journal of Membrane Science. 2009;327(1-2):96-103.
12. Lee Y. Pervaporation of ionically surface crosslinked chitosan composite membranes for water-alcohol mixtures. Journal of Membrane Science. 1997;133(1):103-10.
13. Liu Y-L, Yu C-H, Lee K-R, Lai J-Y. Chitosan/poly(tetrafluoroethylene) composite membranes using in pervaporation dehydration processes. Journal of Membrane Science. 2007;287(2):230-6.
14. Huang RYM, Pal R, Moon GY. Pervaporation dehydration of aqueous ethanol and isopropanol mixtures through alginate/chitosan two ply composite membranes supported by poly(vinylidene fluoride) porous membrane. Journal of Membrane Science. 2000;167(2):275-89.
15. Li B-B, Xu Z-L, Alsalhy Qusay F, Li R. Chitosan-poly (vinyl alcohol)/poly (acrylonitrile) (CS–PVA/PAN) composite pervaporation membranes for the separation of ethanol–water solutions. Desalination. 2006;193(1-3):171-81.
16. Qunhui G, Ohya H, Negishi Y. Investigation of the

permselectivity of chitosan membrane used in pervaporation separation II. Influences of temperature and membrane thickness. Journal of Membrane Science. 1995;98(3):223-32.
17. Shieh J-J, Huang RYM. Pervaporation with chitosan membranes II. Blend membranes of chitosan and polyacrylic acid and comparison of homogeneous and composite membrane based on polyelectrolyte complexes of chitosan and polyacrylic acid for the separation of ethanol-water mixtures. Journal of Membrane Science. 1997;127(2):185-202.
18. Miyata T, Higuchi JI, Okuno H, Uragami T. Preparation of polydimethylsiloxane/polystyrene interpenetrating polymer network membranes and permeation of aqueous ethanol solutions through the membranes by pervaporation. Journal of Applied Polymer Science. 1996;61(8):1315-24.
19. Costa P, Pinto F, Ramos AM, Gulyurtlu I, Cabrita I, Bernardo MS. Study of the Pyrolysis Kinetics of a Mixture of Polyethylene, Polypropylene, and Polystyrene. Energy & Fuels. 2010;24(12):6239-47.
20. Thakur G, Singh A, Singh I. Chitosan-Montmorillonite Polymer Composites: Formulation and Evaluation of Sustained Release Tablets of Aceclofenac. Scientia Pharmaceutica. 2015;84(4):603-17.
21. Katti KS, Katti DR, Dash R. Synthesis and characterization of a novel chitosan/montmorillonite/hydroxyapatite nanocomposite for bone tissue engineering. Biomedical Materials. 2008;3(3):034122.
22. Wang SF, Shen L, Tong YJ, Chen L, Phang IY, Lim PQ, et al. Biopolymer chitosan/montmorillonite nanocomposites: Preparation and characterization. Polymer Degradation and Stability. 2005;90(1):123-31.
23. Tortora M, Vittoria V, Galli G, Ritrovati S, Chiellini E. Transport Properties of Modified Montmorillonite-Poly(e-caprolactone) Nanocomposites. Macromolecular Materials and Engineering. 2002;287(4):243.
24. Chen X, Yang H, Gu Z, Shao Z. Preparation and characterization of HY zeolite-filled chitosan membranes for pervaporation separation. Journal of Applied Polymer Science. 2001;79(6):1144-9.
25. Huang RYM, Pal R, Moon GY. Crosslinked chitosan composite membrane for the pervaporation dehydration of alcohol mixtures and enhancement of structural stability of chitosan/polysulfone composite membranes. Journal of Membrane Science. 1999;160(1):17-30.
26. Jiraratananon R, Chanachai A, Huang RYM, Uttapap D. Pervaporation dehydration of ethanol–water mixtures with chitosan/hydroxyethylcellulose (CS/HEC) composite membranes. Journal of Membrane Science. 2002;195(2):143-51.
27. Kanti P, Srigowri K, Madhuri J, Smitha B, Sridhar S. Dehydration of ethanol through blend membranes of chitosan and sodium alginate by pervaporation. Separation and Purification Technology. 2004;40(3):259-66.
28. Sajjan AM, Jeevan Kumar BK, Kittur AA, Kariduraganavar MY. Novel approach for the development of pervaporation membranes using sodium alginate and chitosan-wrapped multiwalled carbon nanotubes for the dehydration of isopropanol. Journal of Membrane Science. 2013;425-426:77-88.
29. Chanachai A, Jiraratananon R, Uttapap D, Moon GY, Anderson WA, Huang RYM. Pervaporation with chitosan/hydroxyethylcellulose (CS/HEC) blended membranes. Journal of Membrane Science. 2000;166(2):271-80.
30. Dogan H, Durmaz Hilmioglu N. Chitosan coated zeolite filled regenerated cellulose membrane for dehydration of ethylene glycol/water mixtures by pervaporation. Desalination. 2010;258(1-3):120-7.
31. Huang RYM, Pal R, Moon GY. Pervaporation dehydration of aqueous ethanol and isopropanol mixtures through alginate/chitosan two ply composite membranes supported by poly(vinylidene fluoride) porous membrane. Journal of Membrane Science. 2000;167(2):275-89.